energies

MDPI

Article

Fiscal- and Space-Constrained Energy Optimization Model for Hybrid Grid-Tied Solar Nanogrids

Muhammed Shahid [1,2,*], Rizwan Aslam Butt [3,*] and Attaullah Khawaja [4]

[1] Department of Electronics Engineering, NED University of Engineering and Technology, Karachi 75270, Pakistan
[2] Department of Electronic Engineering, Dawood University of Engineering and Technology, Karachi 75270, Pakistan
[3] Department of Telecommunication Engineering, NED University of Engineering and Technology, Karachi 75270, Pakistan
[4] Department of Electrical Engineering, NED University of Engineering and Technology, Karachi 75270, Pakistan
* Correspondence: muhammad.shahid@duet.edu.pk (M.S.); rizwan.aslam@neduet.edu.pk (R.A.B.)

Abstract: Due to rising fossil fuel costs, electricity tariffs are also increasing. This is motivating users to install nanogrid systems to reduce their electricity bills using solar power. However, the two main constraints for a solar system installation are the initial financial investment cost and the availability of space for the installation of solar panels. Achieving greater electricity savings requires more panels and a larger energy storage system (ESS). However, a larger ESS also increases the electricity bill and reduces the available solar power due to higher charging power requirements. The increase in solar power leads to the need for more space for solar panel installation. Therefore, achieving the maximum electricity savings for a consumer unit requires an optimized number of solar panels and ESS size within the available financial budget and the available physical space. Thus, this study presents a fiscal- and space-constrained mixed-integer linear programming-based nanogrid system model (FS-MILP) designed to compute the optimal number of solar panels and ESS requirements, and the daily electricity unit consumption and savings. The proposed model is also validated through an OMNET++-based simulation using real-time solar irradiance and residential load values of one year for the city of Karachi, Pakistan. The investigation results show that a maximum of 1050 electricity units can be saved and exported to the main power grid within the maximum financial budget of PKR 1,000,000/-.

Keywords: nanogrid; integer linear programming; solar panels; electrification

check for updates

Citation: Shahid, M.; Butt, R.A.; Khawaja, A. Fiscal- and Space-Constrained Energy Optimization Model for Hybrid Grid-Tied Solar Nanogrids. *Energies* **2022**, *15*, 8080. https://doi.org/10.3390/en15218080

Received: 31 August 2022
Accepted: 30 September 2022
Published: 31 October 2022

Publisher's Note: MDPI stays neutral with regard to jurisdictional claims in published maps and institutional affiliations.

Copyright: © 2022 by the authors. Licensee MDPI, Basel, Switzerland. This article is an open access article distributed under the terms and conditions of the Creative Commons Attribution (CC BY) license (https://creativecommons.org/licenses/by/4.0/).

1. Introduction

Due to rising fossil fuel costs, the use of renewable energy sources, such as solar and wind turbines, as alternatives, is increasing rapidly. In particular, solar panel costs have decreased gradually during the past 10 years, which has made solar energy a more attractive option as a renewable source [1]. The cost of the electricity is steadily increasing due to the sharp rise in fossil fuel prices in the past 6 months [2]. In contrast, the prices of solar panels are decreasing continuously. Moreover, the solar systems do not create noise and have a long life. Thus, the popularity of solar-based hybrid power systems is steadily increasing [3]. These benefits of solar systems have led to worldwide growth in solar system deployments. According to the recent International Energy Agency (IEA) report of 2021 [4], the European Union installed close to 19.6 GW of solar systems while the rest of Europe added around 2.6 GW, with China being the world leader with 253.4 GW installed. However, developing countries such as Pakistan are facing power shortages, and it has been reported that Pakistan currently has a shortfall of 7000 Megawatts of power. According to the annual report of the National Electric Power Regulatory Authority (NEPRA), 65% of

Pakistan's total electricity generation comes from fossil fuel and 29% from hydroelectric, whereas only 5% comes from renewable energy sources and 1% from other sources [5]. Therefore, solar energy is a very attractive option for electrification in Pakistan, as most of the Pakistan area, especially the southwest, is ideal for solar power generation [6].

The term microgrid is typically used for a solar system powering an industry, a village, or multiple residential units [7]. A microgrid covers a larger area such as an industrial unit or a complete building, with multiple residential units requiring heavy cabling and higher power interfaces. The nanogrid typically covers a single office or residential unit [8]. It manages the power at a smaller level, such as for an office or a single residential unit, and requires a smaller BSS system, a single charge controller, and lighter cabling. Both nanogrids and microgrids can be installed in islanded mode [9] or may be used in ON-Grid mode to supply excess energy to the external power grid. A typical nanogrid is shown in Figure 1. A nanogrid is generally preferable for office or home usage due to its better affordability and simpler maintenance. Generally, a nanogrid is installed for either restoring power in the case of a mains failure or for reducing the electricity bill. In both cases, it requires a suitable sizing and optimization model to accurately compute the required number of solar panels and batteries for the target load.

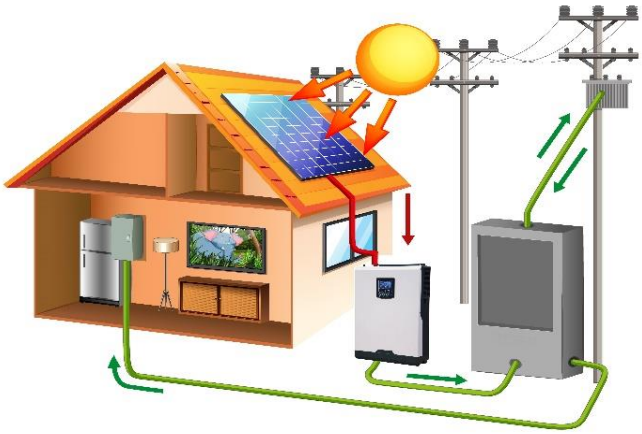

Figure 1. Structure of a typical nanogrid system.

The required number of solar panels and batteries for a nanogrid system can be calculated using basic equations, as shown in ref. [10] and other similar studies, for the target load and battery backup requirements. However, closed-loop nanogrid sizing models are convenient to use and adapt when the design is subject to various constraints, such as peak load power, backup power availability in hours, and available financial budget. An oversized nanogrid solution can meet the target load demands but will not be an economical solution and will also waste the excess unused power [11]. Earlier studies only considered the fiscal constraints and availability, and did not consider the space constraint. However, since the solar panels have a large size, they require a significant horizontal area, and cannot be piled vertically due to the shadowing problem. Thus, the space availability is a big issue. Therefore, this study proposes a fiscal- and space-constrained linear programming (FSLP) model for electrification using a residential hybrid solar nanogrid that minimizes the monthly electricity bill. The mixed-integer linear programming approach is used to develop an optimized closed-loop model.

The rest of the paper is arranged as follows. Section 2 reviews the related work, with a focus on the nanogrid sizing techniques. Section 3 presents the proposed FS-MILP model using the mixed-integer linear programming approach. Section 4 presents the performance evaluation of the proposed model. Section 5 presents the simulation design in OMNET++ for validating the proposed FS-MILP model. Section 6 presents the achievable electricity savings results on a daily and monthly basis under different fiscal constraints. Finally, the

study is concluded in Section 7. Important Notations and descriptions used in rest of the manuscript are summarized in Table 1.

Table 1. Important notations and descriptions.

β	Minimized daily bill of a home
$T_{S_{Hour}}$	Solar panel time of a day in hours
T_{Disc}	Battery discharge time of a day
P_{Batt}	Power of a single battery unit
L_w	AC load of a home
P_{Solar}	Power of a complete solar source
P_{Panel}	Power of a single solar panel
I_{sc}	Short circuit current of solar panel
I_{Pannel}	Actual solar panel current
N_P	No. of solar panels
$T_{Solar\_Day\_Light}$	Sunshine time of a day
I_L	Load current demand
$Batt_{AH}$	Battery ampere hour
V_B	Battery voltage
P_{ESS}	Power of the complete energy storage system
N_B	Total number of batteries in ESS
$T_{K-Electric}$	Time in hours of the end user load being run on the external power provided by K-Electric
V_{CHRG}	Battery charging voltage
Φ_{max}	Maximum saved electricity units by solar nanogrid system
A_{Panel}	Area occupied by a single solar panel
A_{Space}	Total available space at the user premises
C_P	Cost of a single solar panel
C_B	Cost of single battery unit
L_{Budget}	Available budget for solar panels and battery purchase
$Batt_{Min}$	Min. battery ampere hours
$Batt_{AH}$	Capacity of a single battery unit
K_i	Coefficient of short circuit current
T(x)	Temperature of the solar panel surface at time instant x
G(x)	Solar global horizontal irradiation at any time instant x
SoC(t − 1)	Battery initial state of charge
SoC(t)	Battery state of charge at time 't'
Δt	Battery charging time
μ_n	Battery bank capacity
$Units_{ETG}$	Electricity units exported to main power grid
$LOAD_{BE}$	Current drawn from the battery by the inverter when driving the AC load
Eq.	Equation

2. Review of Related Work

Many studies have been presented on the design and performance evaluation of nanogrid systems in different conditions and regions. The first choice for a nanogrid system is to use either a DC, AC [12], or mixed nanogrid design [8]. The DC nanogrid is sensitive to the DC voltage level and it has been reported that a 48 V system is the best choice [13]. For example, the study in ref. [14] presented a DC nanogrid-based smart power distribution infrastructure for a single residential building in Singapore. However, this study was only limited to simulation and no closed-loop model was presented. However, generally, residential systems have mostly AC or mixed loads, so a pure DC system is not feasible. The solar nanogrid system can be deployed on a commercial/industrial scale [5] for power generation, and in residential buildings for electrification [10].

The nanogrid systems can be deployed in a standalone configuration, as presented in ref. [15] and in ref. [16], or in a grid-tied configuration, as shown in ref. [17]. Another recent evolution is the idea of deploying multiple nanogrids instead of a large microgrid, and enabling power sharing among them in a networked manner, which is termed a nanogrid cluster [18]. A detailed study on this idea was presented in ref. [19], which proposes the

resource sharing of battery power and load in a peer-to-peer fashion among the multiple nanogrid units. A distributed generation system in the form of a nanogrid was designed in ref. [20] to fulfil the high energy requirement of self-sufficient buildings. The study monitored the power consumption of individual nanogrid loads in a cloud environment [21]. No control and optimization strategy for the nanogrid was given by the authors. However, clustering is a newer idea and has not gained wide popularity. Generally, the nanogrid systems are installed in a decentralized manner. Many decentralized standalone nanogrid systems have been reported, such as the one implemented for an un-electrified remote village in northeastern India [22]. This is an islanded nanogrid system.

A detailed review of the optimization techniques for solar nanogrid systems was presented in ref. [23]. Some optimization techniques use homogenous algorithms, whereas others use hybrid algorithms, depending on the system design objectives. In the study of [24], the concept of a nanogrid sizing scheme was addressed using an optimization tool termed HOMER. The study assessed the feasibility of a 3.2 KW wind and 4.2 KW solar hybrid nanogrid system in India to drive a maximum load of 2.96 KW. The study concluded that a 2.4 KW solar system was optimal for this scenario. However, no closed-loop sizing model was presented. A similar study was presented for a rural community in northern Nigeria [25]. This study noted that, in nanogrid planning, operational objectives using optimization techniques were also considered, in addition to system sizing and placement.

Most optimization methods implemented in the planning and operations of RE-based power grids use calculus-based, numerical, or static methods, as discussed in ref. [23]. Some of the works that consider either linear programming (LP), integer linear programming (ILP), or mixed-integer linear programming (MILP) are presented in refs. [26–28]. The LP-based algorithms are simple and fast, and offer the provision of optimizing the system subject to various constraints. For example, the study in ref. [29] used the MILP approach for optimizing a solar nanogrid system considering the capital investment and the running maintenance costs. The study in ref. [30] used the MILP approach for optimizing a grid-tied solar microgrid system with minimum line losses. Another optimization algorithm is nested-integer linear programming (NILP). It is used to decompose a large formulation. Simple linear programming (LP) and mixed-integer linear programming (MILP) fail to handle a large number of constraints and variables [28]. A very interesting solar nanogrid optimization technique to minimize initial investment cost was presented in ref. [31]. This study presented the idea of a tenant buying a solar panel and battery from the system administrator to distribute the system investment cost. A detailed review of the solar nanogrid sizing and optimizing techniques is given in ref. [32].

None of the schemes described above consider the space constraint in optimizing the solar nanogrid system. Therefore, in this study, inspired by the optimization approach presented in the grid-tied solar-based system in ref. [33], an MILP approach was chosen for developing a space-, fiscal-, and battery backup-constrained hybrid grid-tied nanogrid model. Similar to [33], the first priority is given to solar power and the deficient energy is imported from the main power grid. The time-of-use concept is used to compute the daily electricity units imported or exported to the main power grid. The study in ref. [34] examined the solar nanogrid system for optimizing the cost of energy and the grid power reliability for the fixed and time-of-use tariffs. A multi-objective optimization technique was also presented in ref. [35] that optimized the solar nanogrid for optimizing the leveled operational cost and the power cut-offs. This study also compared the performance of the MPPT and the PWM charge controllers in terms of nanogrid sizing. However, none of the studies addressed the very important constraint of the space required to install the solar panels, which was addressed in this study.

3. FS-MILP Model for Hybrid Nanogrid System

The nanogrid system was modeled for a typical residential unit comprising AC loads, as shown in Figure 2, with a total instantaneous power consumption of L_w in Kilowatt Hours (KWh). It is assumed that a hybrid inverter is used, with solar having the first power

source priority. Thus, the residential load will be derived from solar power and then from battery power until the battery SOC drops below the 20% value. If the instantaneous power available from the solar panels and the battery bank are P_{Solar} and P_{Batt}, respectively, then the solar panel can drive the residential load for a duration of $T_{S_{Hour}}$ hours and can be represented by Equation (1), where $T_{Solar\_Day\_Light}$ is the sunshine hours of a particular day.

$$T_{S_{Hour}} = [\frac{P_{Solar} - P_{Batt}}{L_w}] * T_{Solar\_Day\_Light} \quad (1)$$

where P_{Solar} and P_{Batt} can be expressed by Equations (2) to (4), respectively.

$$P_{Solar} = N_P * P_{Panel} \quad (2)$$

$$P_{Batt} = N_B * Batt_{AH} * V_B \quad (3)$$

$$P_{Panel} = (\frac{G[x]}{1000} * (180 + (K_i * (T[x] - 298.15))) \quad (4)$$

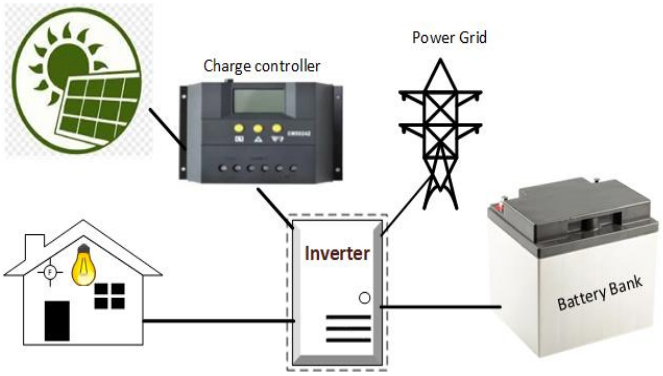

Figure 2. Structure of considered grid-tied nanogrid system.

The solar panel provides electricity while charging the battery at the same time during peak sunshine hours during the day, for 8 h. In the evening and at night, the charged battery will supply electricity until its cut-off point.

Karachi Electric Supply Company (K-Electric) will supply electricity when solar panels and battery are not working. There are two cycles of battery charging in a day. One cycle of battery charging is done by the solar panel and second cycle is done by K-Electric. The discharge time of the battery, T_{Disc}, is the time taken to discharge the battery to a level of 20% of the state of charge (SOC) when it drives the residential load, and can be expressed by Equation (5), where I_L is the current drawn by the load from the battery, which can be expressed by Equation (6). The factor of 0.8 is used to account for the factor of 80% of battery usage to avoid the battery from going into a deep discharge state.

$$T_{Disc} = 0.8 * \frac{N_B * Batt_{AH}}{I_L} \quad (5)$$

$$I_L = \frac{L_w}{V_B} \quad (6)$$

The daily electricity units of the consumer are measured in KWh, and for a residential load can be computed by Equation (7), which also serves as the basis of the objective function for our nanogrid model. The first part of Equation (7) computes the electricity units used of K-Electric power, whereas the second part computes the units consumed in charging the battery, where V_{CHRG} is the battery charging voltage. Here, we assume only a single charging cycle for the battery in a day. $T_{K-Electric}$ represents the time for which the load is run on K-Electric power. This time is computed in Equation (8) by assuming

that, during the daylight duration of $T_{S_{Hour}}$, the solar power is large enough to run the load directly and is computed by Equation (9).

$$\beta = \frac{L_W * T_{K-Electirc} + N_B * Batt_{AH} * V_{CHRG}}{1000} \tag{7}$$

$$T_{K-Electirc} = \left[24 - T_{S_{Hour}} - T_{Disc}\right] \tag{8}$$

$$\begin{aligned} T_{S_{Hour}} &= \left[\frac{P_{Solar} - P_{Batt}}{L_W}\right] * T_{Solar\_Day\_Light} \\ &= \left[\frac{N_P * P_{Panel} - N_B * Batt_{AH} * V_B}{L_W}\right] * T_{Solar\_Day\_Light} \end{aligned} \tag{9}$$

By substituting Equations (8) and (9) into Equation (7) and simplifying, we can write β as Equation (10).

$$\beta = \frac{L_w * 24 - \left[L_w * T_{S_{Hour}} + N_B * Batt_{AH}(0.8V_B - V_{CHRG})\right]}{1000} \tag{10}$$

The objective of this modeling is to minimize the daily electric bill; thus, the objective function θ_{max} can be simply defined by Equation (11) subject to the fiscal and space constraints expressed in Equations (12) to (14).

$$\theta_{max} = L_w * T_{S_{Hour}} + N_B * Batt_{AH}(0.8V_{Batt} - V_{CHRG}) \tag{11}$$

$$N_p * A_{Panel} < A_{Space} \tag{12}$$

$$N_p * C_P + N_B * C_B < L_{Budget} \tag{13}$$

$$N_B > Batt_{Min} \tag{14}$$

The first constraint in Equation (12) limits the solar panel A_{Panel} of N_p to be within the available space at the residential unit, denoted here as A_{Space}. The second constraint Equation (13) ensures that the total cost of the solar panels and the battery bank should not exceed the user budget, denoted here as L_{Budget}, while C_p and C_B denote the cost of a single solar panel and a single battery unit, respectively. The third constraint Equation (14) ensures the computed optimal solution avoids the possibility of making $Batt_{AH}$ too low to minimize the charging cost of the battery bank. Thus, the $Batt_{Min}$ value is chosen to provide a minimum battery backup to the load.

4. Performance Evaluation of the Proposed FS-MILP Model

4.1. Residential Load Profile

For this study, a residential load dataset of one year was considered, available from an earlier study for the residential house units of Lahore, Pakistan [36]. Figure 3 shows the load profile of the house under consideration with an average power consumption of 0.41 KW. The load values were recorded at one-minute resolution daily for the whole year, from 1 January to 31 December.

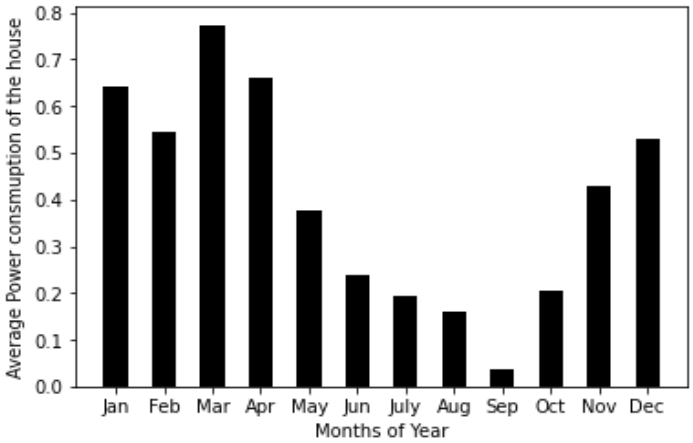

Figure 3. Load profile of the house under consideration.

4.2. Optimization of the FS-MILP Model

The optimized solution of the FS-MILP model depends upon various factors such as irradiance G[x], temperature T[x], and length of the xth solar day, $T_{Solar\_Day\_Light}$, which vary over the year. It also depends upon the fiscal, space, and minimum battery backup constraints. The initial study was conducted for a lower-middle-class family living in a 120 Sq. Yards residential unit, which is the most common residential unit for the middle class, with the assumption that half of the roof space is available for solar panel installation. It was also assumed that a single solar panel has 180 watts rated power and a single battery unit is 200 Ah. We evaluated the model based on average values of each day and the constraint values shown in Table 2.

Table 2. Model parameters and settings.

$Batt_{Min.}$	4 h
L_{Budget}	PKR 200,000/-
C_P	PKR 15,000/-
C_B	PKR 35,000/-
L_w	Shown in Figure 3
P_{Panel}	Shown in Figure 4a
$T_{Solar\_Day\_Light}$	Sunshine time of a day
$Batt_{AH}$	200 Ah
V_B	12 V
A_{Panel}	1.2117771 Sq. Yards
A_{Space}	60 Sq. Yards
V_{CHRG}	15 V
K_i	0.0032

The irradiance and the $T_{Solar\_Day\_Light}$ data for the Karachi region is computed from the data of the solar powered project of World Bank installed in NED University of Engineering and Technology Karachi, Pakistan [20]. For the length of the solar day, the period of the day having a value of irradiance greater than 9 Watt/m^2 is recorded for each day. The average values of the solar power from a single 180-Watts solar panel are derived using Equation (4) and are shown in Figure 4a. The results of the optimized number of 200 Ah batteries and required 180-watt solar panels computed by the model are shown in Figure 4b,c. It is interesting to see that the model provides almost a consistent solution for each day for the constrained budget of PKR 200,000/- and the space constraint of 240 Sq. Yards.

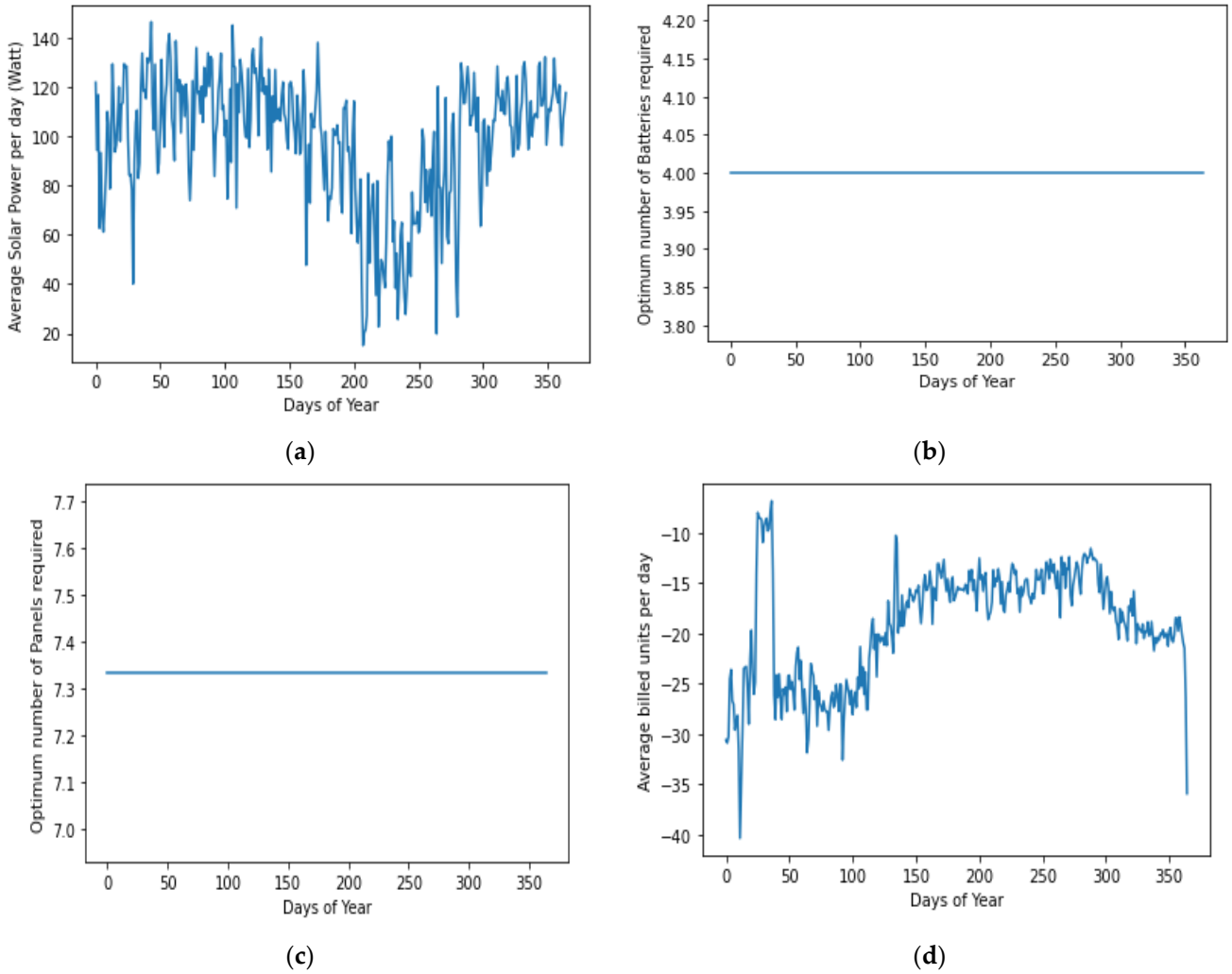

Figure 4. (**a**) Average solar panel power per month; (**b**) optimum no. of required batteries; (**c**) optimum no. of required solar panels; (**d**) avg. expected electricity.

Since the average solar power availability was highest in October, as evident from Figure 4a, with the house load being on the lower side, as evident from Figure 3, maximum energy savings were achieved, as evident from Figure 4c. The negative billed values show excess energy availability that can be exported to the power grid if the grid-tied inverter is used. Thus, with an even higher budget, more energy savings can be achieved and the electricity units can be supplied to the grid. Figure 5 shows the impact of increasing the budget and space on the electricity units that can be saved and the required number of solar panels. It is evident from Figure 5a that increasing the budget beyond PKR 800,000/- has no impact on the saved units, as the required number of panels becomes constant at 50, as evident from Figure 5c, for the R1 type = 120 Sq. Yards residential unit. However, for the R2 type = 240 Sq. Yards residential unit, the electricity unit savings continue to increase until the budget of PKR 1,000,000/-, up to a maximum of 2060 units due to the increase in the number of solar panels to 58, as evident from Figure 5b,d. Thus, space and financial budget both impact the maximum achievable electricity savings. However, the required number of batteries remains the same for a particular backup requirement, which was set to 4 h in this study.

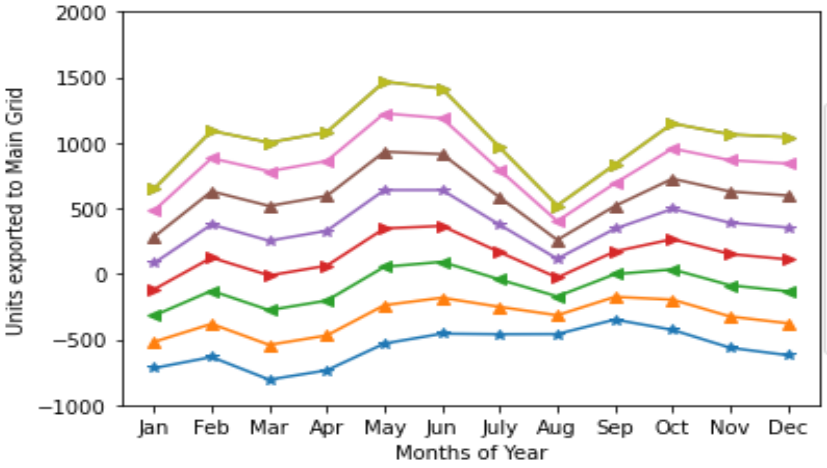

(**a**)

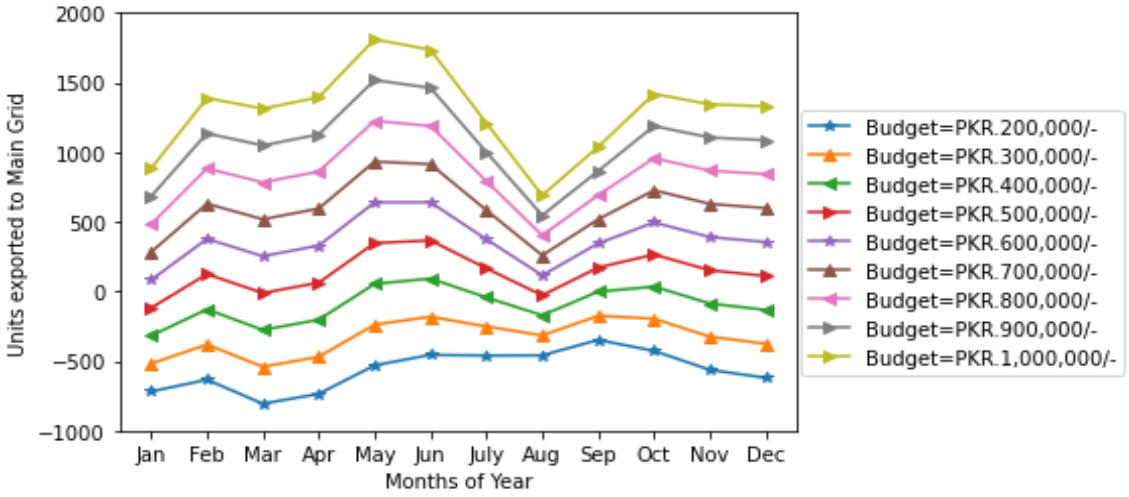

(**b**)

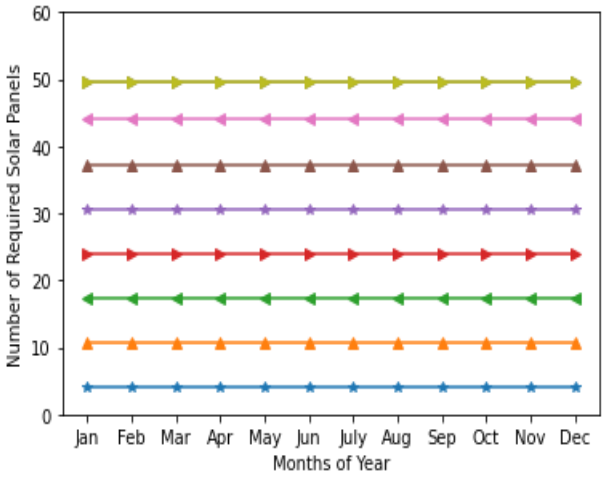

(**c**)

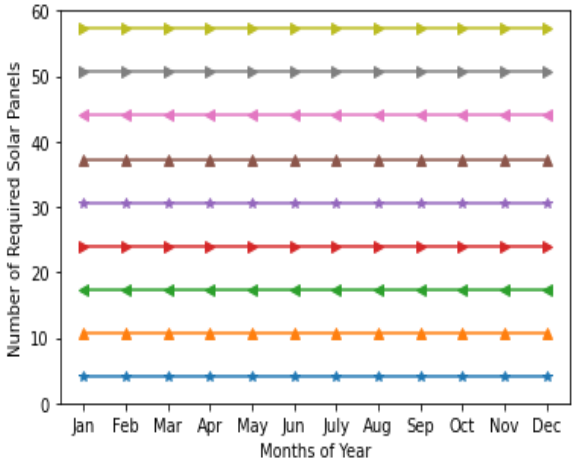

(**d**)

Figure 5. Impact of increasing budget on (**a**) electricity units exported to main grid for R1 house; (**b**) electricity units exported to main grid for R2 house; (**c**) optimized no. of solar panels required for R1 house; (**d**) optimized no. of solar panels required for R2 house.

5. Simulation Design

The nanogrid simulation was implemented using the discrete event simulation environment of OMNET++, comprising a battery, load, solar panel, hybrid inverter, and main power nodes, as shown in Figure 6. The solar panel node was implemented using the real irradiance data from the World Bank project installed in NED University of Engineering and Technology [20]. Equation (15) was used to compute the solar panel output current represented by I_{Pannel} from the solar irradiance and temperature values. In this equation, the panel short circuit is represented by I_{sc}, the coefficient of short circuit current is represented by K_i, the temperature is represented by T, and the solar irradiance is represented by G.

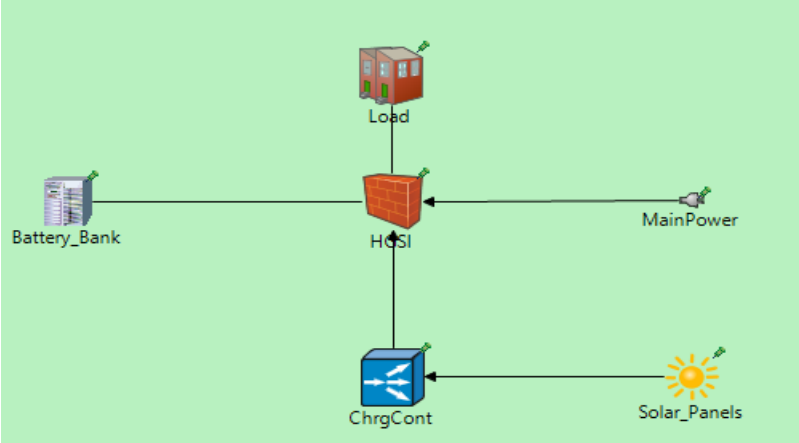

Figure 6. Nanogrid simulation setup in OMNET++.

For the battery node, the state of charge (SoC) of the battery was modeled using Equation (16) based on the Coulomb counting method [37]. In this equation, the battery's initial state of charge is represented by $SoC(t-1)$, battery capacity is represented by μ_n, and battery charging time is represented by Δt.

$$I_{Pannel} = I_{sc} + K_i * (T - 298.5) * \frac{G(x)}{1000} \quad (15)$$

$$SoC(t) = SoC(t-1) - \left[\frac{i_L}{\mu_n} * \Delta t \right] \quad (16)$$

The main role in the nanogrid system is played by the hybrid grid-tied solar inverter (HGSI). The HGSI is configured such that it gives first priority to the solar power, then to the battery power, and finally to the external power source. The working of the HGSI implemented in our simulation is shown with the help of the flowchart shown in Figure 7. It works on four arrival events from the battery, load, solar panel, and update messages. The arrival event from the battery updates the battery SOC level ($BATT_{SOC}$). The arrival event from the load updates the load current and voltage demand variables ($LOAD_I$ and $LOAD_V$, respectively). Similarly, the arrival event from the solar node updates the available current from the solar panel node (I_{PV}). Finally, the update event executes the HGSI process. The HGSI process comprises two main steps. In the first step in every update cycle, the battery is charged, with priority given to solar power. The charging is done at a constant current of 10% using Equation (17). In case the solar power is not enough to meet the required charging current, then the battery is charged from the charger powered by the main power source. However, the charging through main power is only activated if the battery SOC has dropped to the 20% level. In the second step, the load is driven with first priority being the solar power. If the solar power is more than the load power requirement,

Equation (18), then the excess power is exported to the main grid and the electricity units exported to the main grid are computed by Equation (19).

$$\mathrm{BATT_I} = \mu_n * 0.10 * (1 - \mathrm{BATT_{SOC}}) \tag{17}$$

$$\mathrm{Load_{BE}} = \frac{220 * \mathrm{LOAD_I}}{\mathrm{Batt_V}} \tag{18}$$

$$\mathrm{Units_{ETG}} = \frac{\mathrm{I_{PV}} * \mathrm{Batt_V}}{1000 * 60} \tag{19}$$

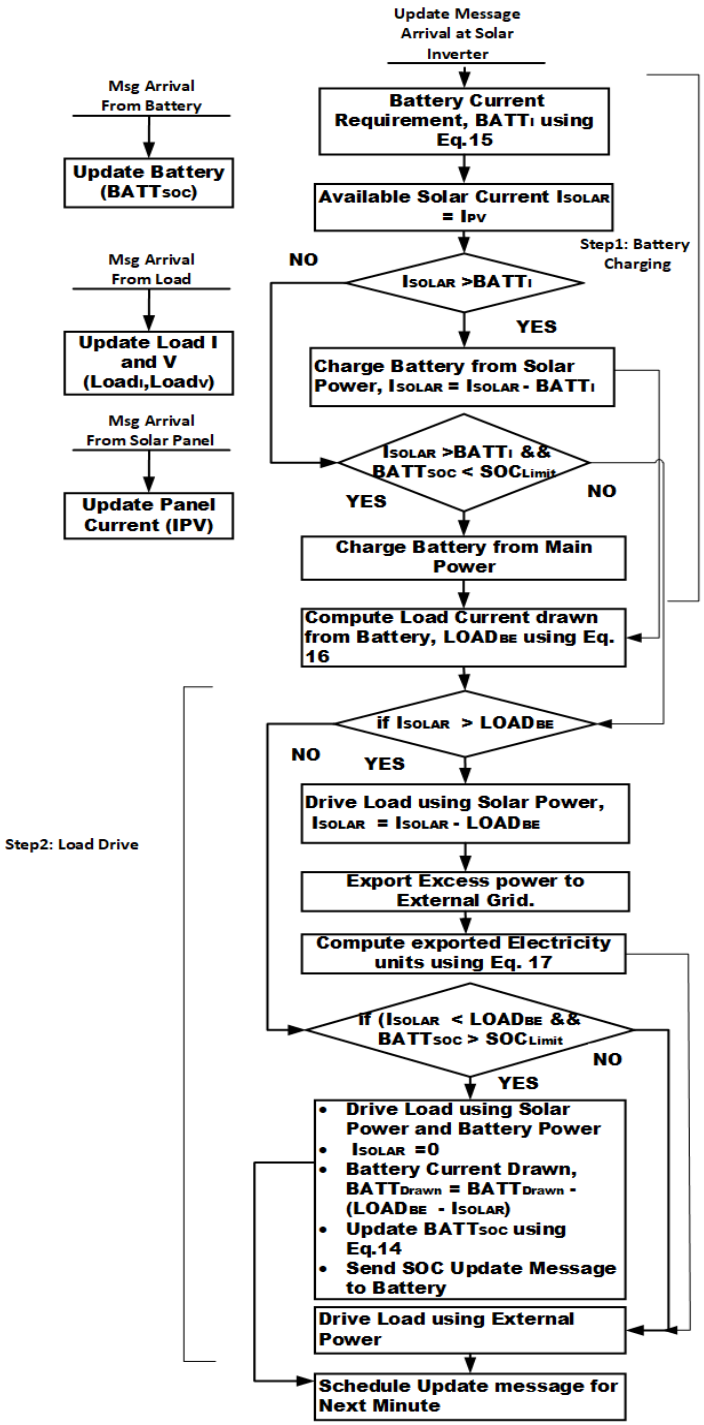

Figure 7. Working process of grid-tied solar inverter node.

The main simulation parameters and settings for the nanogrid setup are shown in Table 3.

Table 3. Simulation parameters and settings.

Simulation Parameter	Values/Source of Data
μ_n	800 Ah
P_{Panel}	180 Watt
Number of Panels	49
Event Timers Expiry time	1 s
SOC_{Lim}	0.2
G(x)	Real-time one-year irradiance data from [20]
Simulation Time	1 Year
AC Load	Real-time house AC load data from [36]

6. Results and Discussions

The daily and monthly electrical units saved or payable to the power operator were computed using the FS-MILP model presented in Section 3. The negative values show that the units were payable by the consumer and the positive values show that the units were exported to the main power grid. For the computation of units from the model, Equation (8) was used and the average daily and monthly values of L_w, $T_{Solar\_Day\_Light}$, T, and G(x) were used. The simulation was run in real time for all of one year and, finally, the daily and monthly values were recorded as vector files. Figures 8 and 9 show the comparison of the status of the daily and monthly units of the consumer.

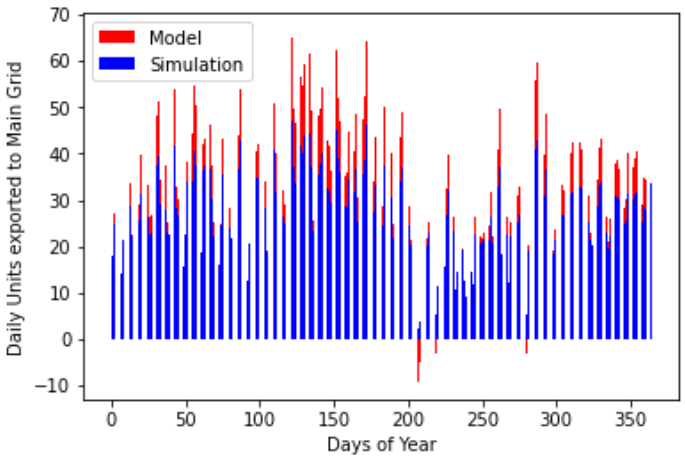

Figure 8. Daily electricity unit savings.

The results obtained are very rational, i.e., the highest savings offered by the solar system are in the months of May and June, as these are the hottest days with full sunshine in the city of Karachi in the summer season. However, by the middle of July to August, it is the rainy season in Karachi, due to which the weather is often cloudy, so the savings achievable by the solar nanogrid are at a minimum. By the end of December and in January, it is the cold season with shorter days, which reduces the solar power. Overall, the simulation and the model results follow the same trend. However, the savings shown by the simulation are lower because it is run on real-time data, whereas the model results are based on the average daily and monthly values.

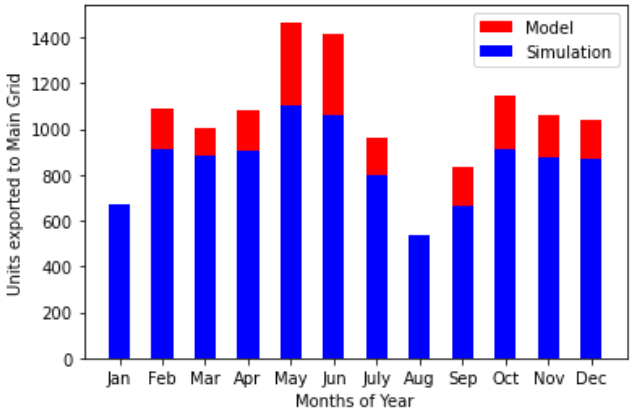

Figure 9. Monthly electricity unit savings.

To evaluate the practical performance of the proposed model, as a case study, we consider the case study of K-Electric and apply its tariff structure [38] to two common types of domestic residential units of R1 = 120 Sq. Yards and R2 = 240 Sq. Yards. K-Electric has a variable and increasing tariff for every 100 units, starting from PKR 13.41/- for 0–100 units and PKR 29.34/- for units above 700, after which it becomes constant. Keeping in view the affordability of the middle class, two budget constraints of PKR 300,000/- and PKR 600,000/- are set for R1, and double these values are set for the R2 type unit. The results of the evaluation from the proposed model are shown in Figure 10. These results show that, for the R1 type, the budget of PKR 300,000/- is not sufficient as it cannot provide any significant savings; rather, it costs extra in the months of May to October due to exceeding the battery charging load and the low solar power availability in these months in Karachi. The budget of PKR 600,000/- provides good financial savings, except in the month of August due to the rainy season. For the R2 type residential unit, the savings increase further due to the higher budget and greater space availability.

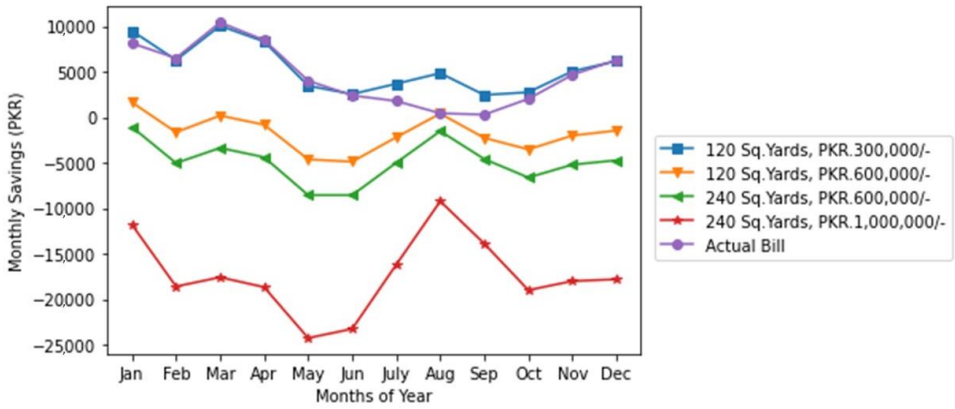

Figure 10. Monthly financial savings due to solar power.

7. Conclusions

A grid-tied nanogrid system model was proposed in this study to minimize the monthly K-Electric bill, and to possibly export the extra electricity units to the main grid. The proposed model can compute the optimized number of required batteries and solar panels subject to the fiscal, space, and time constraints. The model was studied using real one-year solar irradiance data and residential load data of the city of Karachi in Pakistan. The mixed-integer linear programing (MILP) approach was used. The proposed model was also validated through an OMNET++ simulation environment. The simulation and model results show a close correlation. The results show that, even for a 120 Sq. Yards house, a budget of above PKR 300,000/- is required to achieve financial savings from the

solar system. For a budget of PKR 1,000,000/-, up to 1020 units can be exported to the main power grid in the month of May, and a minimum of 500 units can be exported in the month of August. Thus, the electricity savings from the solar system are a function of the financial budget and space. However, a middle-class person living in a 120 Sq. Yards house can also easily reduce their monthly electricity bill with a budget of PKR 600,000/-.

Author Contributions: Conceptualization, R.A.B. and M.S.; methodology, M.S.; software, R.A.B.; validation, A.K. and R.A.B.; investigation, M.S.; resources, R.A.B. and A.K.; Original draft preparation, R.A.B. and M.S.; writing—review and editing, R.A.B. and A.K.; supervision, R.A.B. and A.K. All authors have read and agreed to the published version of the manuscript.

Funding: This study was supported and funded by the NED University of Engineering and Technology, Karachi, Pakistan through its institutional research grant vide order no. Acad/50(48)/977.

Conflicts of Interest: The authors declare no conflict of interest.

References

1. Naing, L.P.; Srinivasan, D. Estimation of solar power generating capacity. In Proceedings of the 2010 IEEE 11th International Conference on Probabilistic Methods Applied to Power Systems PMAPS, Singapore, 14–17 June 2010; pp. 95–100. [CrossRef]
2. Modi, N. Rising costs spell disaster for the nation's health. *BMJ* **2022**, *377*, o938. [CrossRef] [PubMed]
3. Arrinda, M.; Berecibar, M.; Oyarbide, M.; Macicior, H.; Muxika, E.; Messagie, M. Levelized cost of electricity calculation of the energy generation plant of a CO_2 neutral micro-grid. *Energy* **2020**, *208*, 118383. [CrossRef]
4. International Energy Agency. World Energy Outlook 2021: Part of the World Energy Outlook. 2021. Available online: https://www.iea.org/reports/world-energy-outlook-2021 (accessed on 3 October 2022).
5. Ahmed, N.; Khan, A.N.; Ahmed, N.; Aslam, A.; Imran, K.; Sajid, M.B.; Waqas, A. Techno-economic potential assessment of mega scale grid-connected PV power plant in five climate zones of Pakistan. *Energy Convers. Manag.* **2021**, *237*, 11409. [CrossRef]
6. Tahir, Z.U.R.; Asim, M.; Azhar, M.; Amjad, G.M.; Ali, M.J. Hourly global horizontal irradiance data of three stations in Punjab, Pakistan. *Data Brief* **2021**, *38*, 107371. [CrossRef]
7. Nasir, M.; Khan, H.A.; Hussain, A.; Mateen, L.; Zaffar, N.A. Solar PV-Based Scalable DC Microgrid for Rural Electrification in Developing Regions. *IEEE Trans. Sustain. Energy* **2018**, *9*, 390–399. [CrossRef]
8. Cserep, A.; Halasz, A.; Ivancsy, T.; Tamus, Z.A. A nanogrid concept for supplying ICT devices to improve the energy efficiency of small offices. In Proceedings of the 2017 IEEE 2nd Int. Conf. Direct Curr. Microgrids, ICDCM 2017, Nuremburg, Germany, 27–29 June 2017; pp. 440–444. [CrossRef]
9. Azeem, F.; Narejo, G.B.; Shah, U.A. Integration of renewable distributed generation with storage and demand side load management in rural islanded microgrid. *Energy Effic.* **2020**, *13*, 217–235. [CrossRef]
10. Ghafoor, A.; Munir, A. Design and economics analysis of an off-grid PV system for household electrification. *Renew. Sustain. Energy Rev.* **2015**, *42*, 496–502. [CrossRef]
11. Kumar, S.; Krishnasamy, V.; Kaur, R.; Kandasamy, N.K. Virtual Energy Storage-Based Energy Management Algorithm for Optimally Sized DC Nanogrid. *IEEE Syst. J.* **2022**, *16*, 231–239. [CrossRef]
12. Dezfouli, M.; Sopian, K.; Kadir, K. Energy and performance analysis of solar solid desiccant cooling systems for energy efficient buildings in tropical regions. *Energy Convers. Manag. X* **2022**, *14*, 100186. [CrossRef]
13. Moussa, S.; Ghorbal, M.J.-B.; Slama-Belkhodja, I. Bus voltage level choice for standalone residential DC nanogrid. *Sustain. Cities Soc.* **2019**, *46*, 101431. [CrossRef]
14. Jie, L.R.; Naayagi, R.T. Nanogrid for Energy Aware Buildings. In Proceedings of the 2019 IEEE PES GTD Grand International Conference and Exposition Asia (GTD Asia), Bangkok, Thailand, 20–23 March 2019; pp. 92–96.
15. Cairoli, P.; Kondratiev, I.; Dougal, R.A. Controlled power sequencing for fault protection in DC nanogrids. In Proceedings of the 2011 International Conference on Clean Electrical Power (ICCEP), Ischia, Italy, 14–16 June 2011; pp. 730–737.
16. Boroyevich, D.; Cvetkovi, I.; Dong, D.; Burgos, R.; Wang, F.; Lee, F. Future Electronic Power Distribution Systems—A contemplative view. In Proceedings of the 2010 12th International Conference on Optimization of Electrical and Electronic Equipment, Brasov, Romania, 20–22 May 2010; pp. 1369–1380.
17. Tomar, V.; Tiwari, G. Techno-economic evaluation of grid connected PV system for households with feed in tariff and time of day tariff regulation in New Delhi—A sustainable approach. *Renew. Sustain. Energy Rev.* **2017**, *70*, 822–835. [CrossRef]
18. Nasir, M.; Anees, M.; Khan, H.A.; Guerrero, J.M. Dual-loop control strategy applied to the cluster of multiple nanogrids for rural electrification applications. *IET Smart Grid* **2019**, *2*, 327–335. [CrossRef]
19. Lee, S.; Jin, H.; Vecchietti, L.F.; Hong, J.; Park, K.; Son, P.N.; Har, D. Cooperative decentralized peer-to-peer electricity trading of nanogrid clusters based on predictions of load demand and PV power generation using a gated recurrent unit model. *IET Renew. Power Gener.* **2021**, *15*, 3505–3523. [CrossRef]
20. Yerasimou, Y.; Kynigos, M.; Efthymiou, V.; Georghiou, G. Design of a Smart Nanogrid for Increasing Energy Efficiency of Buildings. *Energies* **2021**, *14*, 3683. [CrossRef]

21. Kumar, N.; Vasilakos, A.V.; Rodrigues, J.J.P.C. A Multi-Tenant Cloud-Based DC Nano Grid for Self-Sustained Smart Buildings in Smart Cities. *IEEE Commun. Mag.* **2017**, *55*, 14–21. [CrossRef]
22. Kumar, A.; Deng, Y.; He, X.; Kumar, P.; Bansal, R.C.; Naidoo, R.M. A Renewable based Nano-grid for Smart Rural Residential Application. In Proceedings of the SEST 2021—4th International Conference on Smart Energy Systems and Technologie, Vaasa, Finland, 6–8 September 2021; pp. 1–5. [CrossRef]
23. Al-Falahi, M.; Jayasinghe, S.G.; Enshaei, H. A review on recent size optimization methodologies for standalone solar and wind hybrid renewable energy system. *Energy Convers. Manag.* **2017**, *143*, 252–274. [CrossRef]
24. Tudu, B.; Mandal, K.K.; Chakraborty, N. Optimal design and development of PV-wind-battery based nano-grid system: A field-on-laboratory demonstration. *Front. Energy* **2019**, *13*, 269–283. [CrossRef]
25. Märkle-Huß, J.; Feuerriegel, S.; Neumann, D. Large-scale demand response and its implications for spot prices, load and policies: Insights from the German-Austrian electricity market. *Appl. Energy* **2018**, *210*, 1290–1298. [CrossRef]
26. Mashayekh, S.; Stadler, M.; Cardoso, G.; Heleno, M. A mixed integer linear programming approach for optimal DER portfolio, sizing, and placement in multi-energy microgrids. *Appl. Energy* **2017**, *187*, 154–168. [CrossRef]
27. Cui, H.; Member, S.; Li, F.; Fang, X.; Wang, H.; Chen, H. Bilevel Arbitrage Potential Evaluation for Grid-Scale Energy Storage Considering Wind Power and LMP Smoothing Effect. *IEEE Trans. Sustain. Energy* **2018**, *9*, 707–718. [CrossRef]
28. Urbanucci, L. Limits and potentials of Mixed Integer Linear Programming methods for optimization of polygeneration energy systems. *Energy Procedia* **2018**, *148*, 1199–1205. [CrossRef]
29. Roy, A.; Olivier, J.-C.; Auger, F.; Auvity, B.; Schaeffer, E.; Bourguet, S.; Schiebel, J.; Perret, J. A combined optimization of the sizing and the energy management of an industrial multi-energy microgrid: Application to a harbour area. *Energy Convers. Manag. X* **2021**, *12*, 100107. [CrossRef]
30. Ahmadi, M.; Lotfy, M.E.; Shigenobu, R.; Yona, A.; Senjyu, T. Optimal sizing and placement of rooftop solar photovoltaic at Kabul city real distribution network. *IET Gener. Transm. Distrib.* **2018**, *12*, 303–309. [CrossRef]
31. Olukan, T.A.; Santos, S.; Al Ghaferi, A.A.; Chiesa, M. Development of a solar nano-grid for meeting the electricity supply shortage in developing countries (Nigeria as a case study). *Renew. Energy* **2021**, *181*, 640–652. [CrossRef]
32. Mathew, M.; Hossain, S.; Saha, S.; Mondal, S.; Haque, E. Sizing approaches for solar photovoltaic-based microgrids: A comprehensive review. *IET Energy Syst. Integr.* **2021**, *4*, 1–27. [CrossRef]
33. Dahiru, A.T.; Tan, C.W.; Bukar, A.L.; Lau, K.Y. Energy cost reduction in residential nanogrid under constraints of renewable energy, customer demand fitness and binary battery operations. *J. Energy Storage* **2021**, *39*, 102520. [CrossRef]
34. Hassan, A.; Al-Abdeli, Y.M.; Masek, M.; Bass, O. Optimal sizing and energy scheduling of grid-supplemented solar PV systems with battery storage: Sensitivity of reliability and financial constraints. *Energy* **2021**, *238*, 121780. [CrossRef]
35. Schmid, F.; Behrendt, F. Optimal sizing of Solar Home Systems: Charge controller technology and its influence on system design. *Sustain. Energy Technol. Assess.* **2021**, *45*, 101198. [CrossRef]
36. Nadeem, A.; Arshad, N. PRECON: Pakistan residential electricity consumption dataset. In Proceedings of the 10th ACM International Conference on Future Energy Systems, e-Energy 2019, Phoenix, AZ, USA, 25–28 June 2019; pp. 52–57. [CrossRef]
37. Nasir, M.; Jin, Z.; Khan, H.A.; Zaffar, N.A.; Vasquez, J.C.; Guerrero, J.M. A Decentralized Control Architecture Applied to DC Nanogrid Clusters for Rural Electrification in Developing Regions. *IEEE Trans. Power Electron.* **2018**, *34*, 1773–1785. [CrossRef]
38. Karachi Electric Supply Corporation. Tarrif Structure of KESC. *Tarrif Struct.* 2022. Available online: https://www.ke.com.pk/customer-services/tariff-structure/ (accessed on 15 September 2022).